Int. J. Heat Mass Transfer. Vol. 15, pp. 1553–1567. Pergamon Press 1972. Printed in Great Britain

A CRITICAL EXAMINATION OF THE VALIDITY OF SIMPLIFIED MODELS FOR RADIANT HEAT TRANSFER ANALYSIS

J. S. TOOR and R. VISKANTA
Heat Transfer Laboratory, School of Mechanical Engineering, Purdue University, Lafayette, Indiana 47907, U.S.A.

(*Received* 2 *August* 1971 *and in revised form* 22 *November* 1971)

Abstract—The validity of the commonly used simplified models for predicting local as well as overall radiation interchange among real surfaces has been critically examined. The directional and spectral effects have been examined by comparing the experimental data with the predictions based on six simple models for the radiation characteristics of surfaces. The directional property variations were evaluated from Fresnel's equations with the optical constants predicted from simple Drude's theory.

The configuration studied consisted of three plane parallel surfaces of finite extent. This permitted critical examination of the influence of various parameters on radiation interchange. The test surfaces were gold with rms roughnesses varying from 0·02 μ to 7·1 μ. Enclosure surface temperatures varied from 77°K to 760°K. The local incident flux was measured on the total basis. The prediction of the overall irradiation using appropriate constant property models agrees well with the experimental results to within the combined experimental and theoretical uncertainties. In general, the analysis and experiment agree better for prediction of local irradiation when the directional property variation and specularity of surfaces is taken into account. The experimental data agree equally well with the gray and semigray analyses in which the directional effects are considered and the direction independent specular component of reflectance is calculated by taking into account the spectral, directional and configuration effects.

NOMENCLATURE

A, surface area;
a_m, mechanical correlation distance;
B, bidirectional;
B_{di-j}, local absorption factor defined as the fraction of energy emitted from an elementary area dA_i and absorbed at surface A_j (directly and indirectly after all possible inter-reflections in the enclosure);
D, diffuse;
CP, constant property;
DP, directional property (emission and absorption according to Fresnel's equations);
E_{abs}, rate of energy absorption;
E, total energy emitted per unit time and per unit area;
EXP, experimental;
G, irradiation;
I, intensity of radiation;
L, W, H, see Fig. 1;
N, number of surfaces in the enclosure;
Q, overall (average) heat-transfer rate;
q, local heat flux;
S, specular;
S-1, specular surface 1;
S-B-S, surfaces in positions 1, 2 and 3, respectively;
T, temperature;
UR, uniform radiosity;
x, y, z, coordinates.

Greek symbols
α, absorptance, absorptivity;
γ, δ, H/L and W/L, respectively;

E

ε, emittance, emissivity;
θ, polar angle;
λ, wavelength;
μ, micron,
ξ, η, dimensionless coordinates x/L and y/L, respectively;
ρ, reflectance, reflectivity;
σ_m, mechanical r.m.s. roughness;
ϕ, azimuthal angle;
Ω, solid angle;
$\mathbf{\Omega}$, unit vector denoting the direction (θ, ϕ) of radiation.

Subscripts
b, refers to blackbody;
G, gray;
i, j, dummy indices;
SG, semigray;
λ, refers to spectral values;
$\cap$, integration over hemisphere.

Superscripts
d, diffuse component of reflectance;
s, specular component of reflectance;
$*$, dimensionless, i.e. $G^* = G/\varepsilon E_b$;
$'$, refers to incident.

INTRODUCTION

THERMAL problems encountered in the design of space vehicles capable of penetrating into unfamiliar environment include such widely divergent areas as long-life storage of cryogenic liquids, heat rejection systems, solar power generation devices, maintenance of safe and comfortable environments in living quarters and instrument compartments. In these and many other applications radiation heat transfer is quite important and in some cases it is the only mode of energy transfer. Other areas where knowledge of radiant heat transfer is essential involve the design of furnaces, high temperature equipment, high temperature energy conversion devices. The inability to accurately predict radiant heat transfer has been illustrated by overheating of many spacecrafts which has lead to failure of costly experiments. Future generation spaceships with tighter thermal tolerances and much longer active life will demand improved thermal design and control. The particular applications have called for more reliability, greater precision and greater detail in radiant heat transfer predictions than were considered necessary in the past.

This demand has provided the impetus for the research effort in the various aspects of radiant heat transfer; however, experimental studies have been few and only a modest amount of more detailed analyses has been reported. Predictions of radiation interchange have been limited to simple surface characteristics models and enclosures because of the complexity of the problem and the lack of accurate knowledge of radiation properties of surfaces. However, the validity of these simple models has not been substantiated by more refined analyses or experiments. The small number of experiments carried out have reported the measurements on a total (integrated over the whole spectrum) basis only. The experimental data on local basis are not conclusive and in some cases are contradictory [1–4]. However, these conclusions are based on the comparison of measured total heat transfer with gray or semigray analysis. This shows the need for additional research effort so that appropriate comparisons can be made, i.e. comparison of spectral measurements with spectral analysis and of total measurements with nongray analysis.

This study is undertaken to meet this need. Specifically, the purpose is to critically examine the validity of the commonly used simplified models for predicting local as well as overall radiation interchange among real surfaces on total basis. The directional effects are examined by comparing the experimental data with the predictions based on simple and more detailed models for the radiation characteristics of surfaces. In this paper only the comparison of results on total basis is reported. The spectral results and the details of the experiment can be found elsewhere [5].

ANALYSIS

Formulation of problem

The radiation heat exchange in an enclosure (accounting for the spectral, directional and surface roughness effects) can be formulated with as few idealizing assumptions as possible using the integral or the Monte Carlo methods. The integral method was found to be impractical even on a fast digital computer (CDC 6500) and was abandoned in favor of the Monte Carlo method. Hence, the problem is formulated and the calculations are performed using the Monte Carlo method.

In the analysis it is assumed that the geometric optics theory is valid for radiant heat-transfer analysis between surfaces separated by a nonparticipating medium having an index of refraction of unity. In addition the polarization effects are ignored. All the radiant heat-transfer quantities of interest such as the heat flux, radiation interchange or irradiation can be readily calculated, once the absorption factors B_{di-j}'s are calculated [6].

The energy absorbed at the elementary area dA_i due to emission from all the N surfaces in the enclosure can be expressed as

$$E_{abs} = \sum_{j=1}^{N} A_j \varepsilon_j B_{j-di} E_{bj} \tag{1}$$

and the local radiant heat flux is given by

$$q_i = dQ_i/dA_i = \varepsilon_i E_{bi} - \left[\sum_{j=1}^{N} A_j \varepsilon_j E_{bj} B_{j-di}\right]/dA_i. \tag{2}$$

It follows from equation (1) that the irradiation at dA_i is

$$G_i = \sum_{j=1}^{N} A_j \varepsilon_j E_{bj} B_{j-di}/\alpha_i dA_i \tag{3}$$

where ε_j and α_i are the hemispherical emissivity and absorptivity, respectively, and are defined as

$$\varepsilon = \frac{\int_0^\infty \int_\Omega \varepsilon_\lambda(\boldsymbol{\Omega})\, I_{b\lambda} \cos\theta \, d\Omega \, d\lambda}{\int_0^\infty \int_\Omega I_{b\lambda} \cos\theta \, d\Omega d\lambda} \tag{4}$$

$$\alpha = \frac{\int_0^\infty \int_{\Omega'} \alpha_\lambda(\boldsymbol{\Omega}')\, I'_\lambda(\boldsymbol{\Omega}') \cos\theta' \, d\Omega' \, d\lambda}{\int_0^\infty \int_{\Omega'} I'_\lambda(\boldsymbol{\Omega}') \cos\theta' \, d\Omega' \, d\lambda}. \tag{5}$$

The calculation of radiant energy quantities from the above relations is straight forward after the required factors B_{j-di} and the hemispherical absorptivities α_i are calculated. The absorption factor B_{j-di} can be calculated from the spectral values $B_{\lambda j-di}$ or obtained directly. The former method is very cumbersome and usually the latter is used. The details of the calculations using the Monte Carlo method can be found elsewhere [6, 7]. Unfortunately, on total basis the reciprocity relation

$$dA_i \varepsilon_i B_{di-j} = A_j \varepsilon_j B_{j-di} \tag{6}$$

in general is not valid. This relation is useful because with its help equations (1)–(3) can be put in a more convenient form. For gray surfaces use of the reciprocity relation yields

$$E_{abs} = \sum_{j=1}^{N} dA_i \varepsilon_i B_{di-j} E_{bj} \tag{7}$$

$$q_i = \varepsilon_i \left[E_{bi} - \sum_{j=1}^{N} E_{bj} B_{di-j}\right] \tag{8}$$

$$G_i = \sum_{j=1}^{N} \varepsilon_i E_{bj} B_{di-j}/\alpha_i. \tag{9}$$

Equations (7)–(9) have been purposely cast in this form because now the radiant energy quantities can be calculated more efficiently. In the Monte Carlo calculations it is advantageous to predict B_{di-j} rather than B_{j-di} because the local radiant quantities can be calculated directly at a few points of interest. For gray surfaces all the B_{di-j}'s can be evaluated simultaneously resulting in considerable saving of computer time. In general, $B_{di-j} \gg B_{j-di}$ and it is on this fact that the accuracy of the Monte Carlo method depends. The larger the B_{di-j}, the more accurate is the result for the same number of energy bundles traced. Also some of the short cuts [6] can be used more fruitfully for a single point than for an entire area.

Use of equation (9) to predict the irradiation presents two difficulties: (1) The relation is valid only for gray surfaces, or equal temperatures of surfaces i and j, and (2) it is not easy to calculate

α because its evaluation demands the knowledge of the incident radiation field. However, the second difficulty can be by-passed if the absorption factors B_{di-j} are calculated by considering emission from dA_i as diffuse. This amounts to introducing at the desired location a fictitious surface dA_i having constant properties and reduces equation (9) to

$$G_i = \sum_{j=1}^{N} E_{bj} B_{di-j}. \qquad (10)$$

It is evident that the introduction of this fictitious surface dA_i does not alter the character of the enclosure because in all the interreflections it is the real surface which participates in the radiation interchange. The first difficulty can also be overcome easily. It has been proven [8] that equations (6)–(9) are also valid on nongray basis provided that in calculating the absorption factors B_{di-j} the energy emitted from dA_i corresponds to radiation characteristics of dA_i at temperature T_i, but the blackbody emission corresponds to temperature T_j.

Radiation characteristics of surfaces

An analysis of radiation exchange among surfaces requires an acceptable description of the radiation characteristics of surfaces. The degrees of detail required in specifying the radiation characteristics, i.e. emission, absorption and reflection, depend upon the surface arrangement, temperatures, emissivities and the energy quantities to be calculated. For example, the calculation of the local (overall) radiant heat loss, as compared to local (overall) radiant interchange, may demand a different degree of detail of the radiation characteristics of surfaces.

In the present application, where an attempt is made to evaluate the importance of real surface effects, considerable detail is required in specifying the radiation properties. However, the intent here is to adopt simple models that predict the radiant heat exchange realistically rather than to calculate the radiant exchange from more complicated models. Previous studies [1–4] have shown that for better accuracy in the prediction of radiant interchange, directional effects must be taken into account. However, these calculations are based on gray or semigray analyses. The predictions based on nongray directional property models for infinite parallel plates in some cases were higher by a factor of four [9], which illustrates the importance of spectral and directional effects. Hence, for a meaningful comparison of the experimental data and the predictions the dependence of radiation characteristics on direction, wavelength, temperature, and surface roughness should be accounted for accurately. This, however, requires precise knowledge of the optical constants of the surface materials. In a recent study Bennett and Bennett [10] have shown that the measured infrared reflectance from carefully prepared high conductivity materials like silver, gold and aluminum surfaces is in excellent agreement with the predictions of Drude's theory in the infrared spectrum.

Commercial surfaces are rarely ideal, i.e. clean and optically smooth. It has been reported that emittance of pure metals (clean) is smaller [11, 12] than those deposited commercially, due to contamination and surface damage. The effect of roughness on the directional characteristics can be found elsewhere [13, 14]. It suffices to say that slight roughness ($\sigma/\lambda \ll 1$) does not materially affect the magnitude of absorptance and emittance; however, it strongly influences the spatial distribution of the reflected energy.

The slightly rough surface ($\sigma/\lambda \ll 1$), has been studied in detail by Houchens and Hering [13]. They have examined the Davies and the Beckmann [15] models for predicting the spatial distribution of reflected energy. Both of the models assume that the surfaces are randomly rough and can be described statistically by the normal distribution of the surface heights and the autocorrelation coefficient. Electrical conductivity of the material is assumed to be infinite, i.e. it is perfectly reflecting. They have shown that the predictions of the Beckmann model compare favorably with the experimental data [16, 17]. One of the limitations of this model is that, to account for the finite conductivity of materials, the reflection distribution function is multiplied by the reflectance of the optically smooth material. Although this approximation violates Helmholtz reciprocity relation in the incoherent part of reflection distribution function, it predicts the bidirectional reflectance reasonably well [13, 17]. Use of the incoherent part of the reflection distribution function, however, is too complicated for engineering calculations [3, 18], and such a detailed analysis is not justified in view of the fact that radiation characteristics of surfaces in general are not known accurately enough.

Since consideration of spectral effects makes the problem rather complicated it is felt that for engineering calculations alternative simple models should be explored. It should be based on the properties which can either be easily measured or can be calculated by incorporating the important spectral and directional effects. The predictions based on simplified models, then, must be compared with the predictions of nongray calculations and the experimental data to check the validity of the analysis. The models used in the analysis are summarized in Table 1.

The radiation properties used in nongray analysis are spectral properties. The total directional absorptances are calculated with the spectral distribution of the incident flux corresponding to the emitting surface. Thus, for calculating B_{di-j}, $\alpha_i(\theta')$ is evaluated from the equation

$$\alpha_i(\theta') = \int_0^\infty \alpha_\lambda(\theta', T_i) E_{b\lambda}(T_j) \mathrm{d}\lambda / E_b(T_j). \quad (11)$$

The specular component of reflectance used in nongray calculations is predicted from the coherent component of Beckmann model. i.e.

$$\rho^s(\theta', \sigma/\lambda) \simeq \rho_\lambda(\theta') \exp\{-[4\pi(\sigma/\lambda)\cos\theta']^2\}. \quad (12)$$

For semigray and gray analyses with the $D + S$ model the specular component of reflectance is independent of direction but it takes into account the spectral and directional effects as well as the geometry. The details of the calculations are omitted to conserve space and can be found in [8].

Configuration, surface materials and surface roughness

The configuration chosen for the study consisted of three square plates arranged as shown in Fig. 1. The choice of the configuration was dictated by previous studies which showed that, with surfaces of finite extent, it yields a very critical comparison between the predictions of the various models. Some of the other reasons are: The configuration has a simple geometrical character, is suitable for experiment and analysis and it can be made to represent both open and closed systems by easy change of parameters. This configuration was recommended by Bobco [19] also for experimental study.

Table 1. Theoretical models for radiation characteristics of surfaces

Symbol	Emission and absorption	Reflection	Analysis
	Constant property models		
D	Diffuse	Diffuse	Gray
S	Diffuse	Specular	Gray
$D + S$	Diffuse	Diffuse + Specular	Gray
	Directional property models		
$DP(S)$	Directional	Specular	Nongray, gray
$B(D + S)$	Directional	Specular + Diffuse	Nongray
$DP(D + S)$	Directional	Specular + Diffuse ($\rho^d(\theta')/\rho(\theta')$ = constant)	Gray

Previous studies [1, 4] had shown that it is for highly reflecting materials that the choice of the model is more critical. For this reason, gold was chosen as a test surface material as it satisfies the experimental requirements, i.e. is stable at high temperatures, has low vapor pressure, and does not tarnish in air. Also the radiation characteristics of gold could be predicted [10] accurately from Drude's theory.

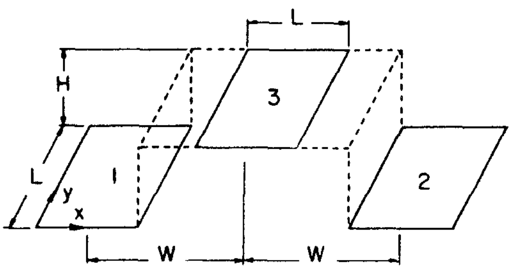

FIG. 1. Configuration studied.

The choice of surface roughness was guided by the desire to cover the whole range of specular component (zero to one). The rough ness of test-specimen reported in Table 2 is a mean of measurements at five locations on a surface 15·24 cm square. The maximum departure from the mean was about six per cent. The surfaces were found to be isotropic. Although autocorrelation coefficient showed normal distribution the surface height density departed from the Gaussian [5].

EXPERIMENT

In the experiment only the measurement of temperature and irradiation was required. Irradiation was measured by thermopiles at eight locations in the cold surface 1. The thermopiles were 6 mm in diameter, uncompensated, evacuated and were of the end on pencil type with KBr windows. The experiment was conducted inside a double walled aluminum environment chamber painted black on the inside. The chamber was cooled by LN_2 (77°K) to effectively eliminate any radiant energy external to the test surfaces. During the experiment the pressure inside the chamber was reduced to $1{\cdot}33 \times 10^{-2}$ N/m^2 or less. This practically eliminated convection and helped in obtaining uniform temperature over the test surfaces. Full details of the experiment are given elsewhere [5].

RESULTS AND DISCUSSION

Parameters

There is, of course, an infinite number of combinations of the various independent parameters, and so it is necessary to be selective. The reasons for selecting the particular configuration used have already been given. The dimensionless separation distance δ was maintained close to unity while the dimensionless spacing γ between the plates was kept at $\frac{1}{6}$ to $\frac{1}{2}$. This choice of the parameters was dictated by irradiation consideration on the detectors as well as the available space in the chamber. For

Table 2. Description of surfaces and the measured roughness

Designation of surfaces	Roughness $\sigma_m(\mu)$ radius of stylus 2·5 μ	Roughness $\sigma_m(\mu)$ radius of stylus 12·5 μ	Correlation distance $a_m(\mu)$	Method of preparation. Goldplated after being:
S-1	0·02	—	—	Polished
S-2	0·03	—	—	Polished
S-3	0·02	—	—	Polished
B-2	1·50	0·90	40·0	Blasted with glass beads
B-3	0·75	0·50	14·0	Blasted with glass beads
D-3	7·10	5·50	25·0	Blasted with steel grit

each spacing the data were taken at two temperature levels of the hot surface 2. The higher temperature level was limited by experimental requirements. The cold surface was maintained at about room temperature. This was necessary for good performance of the thermopiles which passed through the cold block. Surface 3 was kept at the LN_2 temperature (77°K) for two reasons. Firstly, at this temperature the emission from this surface can be neglected thus simplifying the predictions. Secondly, because the absorptance of gold at this temperature is very small the surface is practically adiabatic. Previous studies [4] have shown that it is in the presence of an adiabatic surface in an enclosure that a large discrepancy occurs between experiment and analysis.

For a meaningful comparison of the experimental and analytical results the radiation characteristics of surfaces must be known to an acceptable accuracy. After carefully examining the available data, including that compiled by the Thermophysical Property Research Center of Purdue University [20], values of the total hemispherical emittance were selected which corresponded to samples prepared in a manner similar to those used in this study. Complete bidirectional data could not be found in the literature. In view of the lack of needed radiation property data, the values used in the analysis are based on those predicted by Fresnel's equations. The optical constants were calculated by the simple Drude theory. The values predicted by Fresnel's equations were proportioned to yield the selected experimental total hemispherical emittance.

The accuracy of the Monte Carlo program was checked in some cases by comparing these results with those predicted from the integral equation solutions. The comparison was found to be very good. Since the Monte Carlo method is a statistical one, the results did have some scatter, but it was small. The curves shown in the figures were faired through the plotted points corresponding to the values calculated by means of the Monte Carlo method.

Before discussing the results it is appropriate to examine the local irradiation at surface 1 due to emission from other surfaces. Rewriting equation (10) in dimensionless form yields,

$$G_1^* = [B_{d1-1} + B_{d1-2}(T_2/T_1)^4 + B_{d1-3}(T_3/T_1)^4]/\varepsilon_1. \qquad (13)$$

It is clear from equation (13) that the irradiation depends on the absorption factors and the temperatures. When B_{di-j} are of the same order of magnitude the main contribution to G_1^* is from B_{d1-2} when $(T_2/T_1)^4$ is large. In the present study $(T_3/T_1)^4 \simeq 0.005$ and $(T_2/T_1)^4$ varies approximately from 20 to 50. In such a case (for all B_{di-j} equal), ignoring B_{d1-3} results in a difference of less than 0.025 per cent. For large values of $(T_2/T_1)^4$ even B_{d1-1} may be ignored. For example, a difference of less than 2 per cent (when B_{d1-1} and B_{d1-2} are equal) results in the value of G_1^* for $(T_2/T_1)^4 = 50$. Hence, in the calculations the emission from surface 3 was justifiably neglected. Some sample results are presented in Fig. 2 to illustrate the order of magnitude of the absorption factors. The key to the

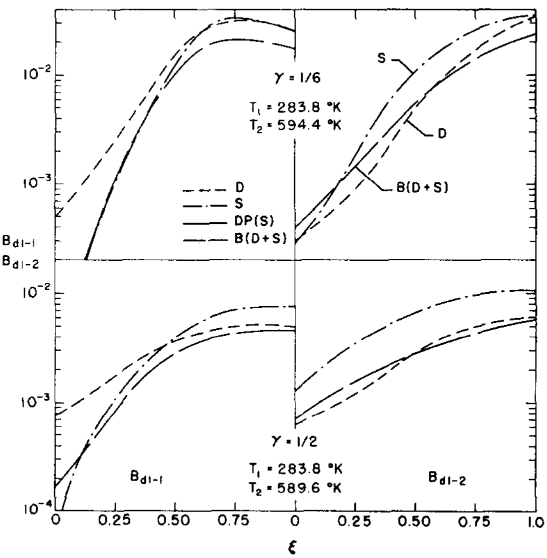

FIG. 2. Comparison of local absorption factors for different models; surface arrangement S-S-B. $\delta = 1$, $\eta = \frac{1}{8}$.

Table 3. Overall measured irradiation and fractional departure from experiment for various analyses on total basis

Surfaces 1-2-3	γ	T_1 °K	T_2 °K	G^*_{EXP}	UR	(Analysis-Experiment)/Experiment S	D	$D+S$	$DP(S)$	$B(D+S)$	$DP(S)_{SG}$	$DP(S)_G$	$DP(D+S)_{SG}$	$DP(D+S)_G$
S-S-S	$\frac{1}{6}$	284·2	597·3	9·64	−0·19	0·04	−0·14		−0·11			−0·08		
		285·2	761·9	28·71	−0·20	0·00	−0·18		−0·13		−0·11	−0·09		
	$\frac{1}{2}$	283·5	577·8	3·81	−0·36	−0·02	−0·43		−0·21			−0·20		
		284·6	746·8	11·77	−0·35	−0·01	−0·44		−0·20		−0·16	−0·18		
S-S-D	$\frac{1}{6}$	283·7	595·7	6·78	0·15	0·10	0·21		−0·03		0·00	0·00		
		283·6	756·8	19·80	0·16	0·07	0·18		−0·05		−0·02	−0·01		
	$\frac{1}{2}$	283·6	580·6	2·03	0·23	0·07	0·08		−0·16		−0·12	−0·05		
		284·2	752·9	6·41	0·25	0·07	0·08		−0·15		−0·11	−0·10		
S-S-B	$\frac{1}{6}$	283·8	594·4	7·39	0·04	0·36	0·15	0·06		−0·14				
		283·7	763·3	23·11	0·03	0·31	0·10	0·04		−0·20			−0·12	−0·11
	$\frac{1}{2}$	283·8	589·6	2·02	0·32	1·07	0·14	0·40		0·04				
		283·9	756·1	5·80	0·41	1·21	0·20	0·41		0·05			0·22	0·21
S-B-S	$\frac{1}{6}$	283·9	589·4	7·49	−0·01	0·28	0·09	0·07		−0·17				
		284·8	759·2	23·20	−0·01	0·25	0·05	0·03		−0·19			−0·10	−0·09
	$\frac{1}{2}$	284·8	755·4	9·40	−0·14	0·34	−0·27	0·12		−0·13			−0·09	−0·09
S-B-B	$\frac{1}{6}$	283·8	594·9	8·06	−0·04	0·25	0·06	−0·00		−0·20				
		284·3	758·2	22·77	0·00	0·28	0·07	−0·04		−0·20			−0·11	−0·10
	$\frac{1}{2}$	284·1	582·1	2·24	0·12	0·76	−0·03	0·18		−0·16				
		284·5	750·4	6·68	0·17	0·84	−0·00	0·17		−0·14			−0·05	−0·05

various lines on all the figures is the same as that given in Fig. 2. It is clear that the order of magnitude of B_{d1-1} and B_{d1-2} at corresponding points is the same. Since $(T_2/T_1)^4 \gg 1$ it was expected that the trend of the irradiation curves should be similar to those of B_{d1-2}, which was confirmed later.

All the data presented are in terms of total irradiation at the cold surface. They have been nondimensionalized with respect to the total emissive power of the cold surface. In the presentation of the data the subscript 1 has been dropped for convenience since all the data are for surface 1. The overall (average) irradiation results presented in Table 3 were obtained from the local values.

Comparison of measured and predicted local irradiation

In Fig. 3 the analytical predictions for the constant property diffuse, specular, and directional property specular *DP*(*S*) (nongray) models of irradiation are compared with the experimental data (circles) when all the surfaces are "specular" ($\sigma_m < 0{\cdot}03\mu$). Examination of the figures reveals that the experimental data are in best agreement with the predictions of *DP*(*S*) analysis; however, at some points these predictions are about 20 per cent lower than the data. The results based on diffuse analysis are about 70 per cent lower than the experimental data. At both temperature levels, for Figs. 3 and 4, the predictions of the diffuse analysis are always lower than those of the constant property specular analysis. Since the local heat flux at the cold surface is given by

$$q_1^* = 1 - \varepsilon_1 G_1^* \tag{14}$$

this means that the diffuse analysis would predict too high a heat flux. The lower irradiation shows that more of the energy leaves the enclosure for the diffuse than for the specular reflection model. This is typical of enclosures which exchange a large portion of their energy in near normal directions. As an example, for two parallel plates with a large separation distance, the irradiation based on the specular model is always higher [1, 6] than that based on the diffuse model. This seems plausible because at each reflection from a diffuse surface the energy

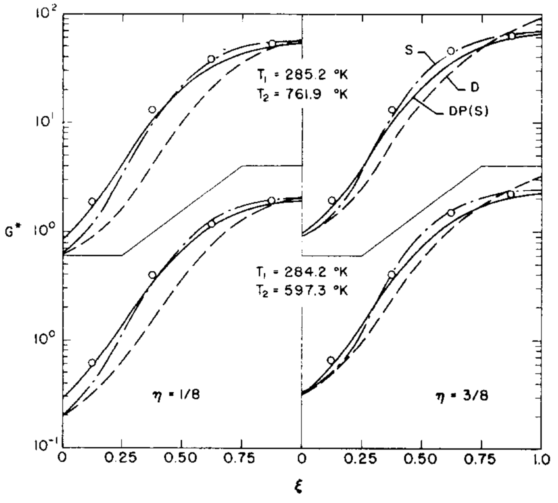

FIG. 3. Comparison between measured and predicted local irradiation for different models; surface arrangement *S-S-S*, $\delta = 1$, $\gamma = \frac{1}{6}$.

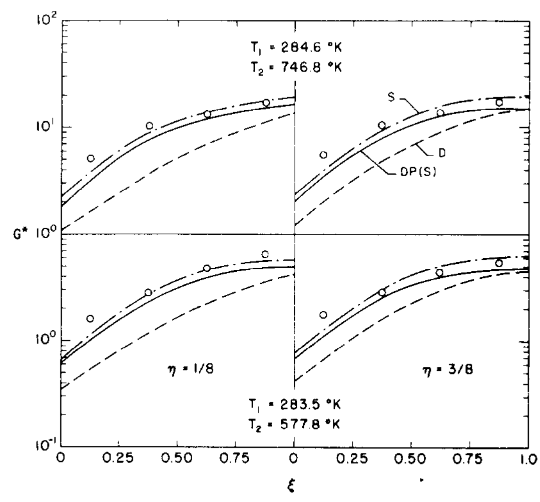

FIG. 4. Comparison between measured and predicted local irradiation for different models; surface arrangement *S-S-S*, $\delta = 1$, $\gamma = \frac{1}{2}$.

is uniformly distributed with a constant intensity. On the other hand, when more of the energy exchange occurs in directions other than the normal, the diffuse analysis would predict higher irradiation. This conclusion is supported by calculations of the adjoint plate system [6, 21].

For the "specular" enclosure with a spacing of $\gamma = \frac{1}{2}$ (Fig. 4) strangely enough the data show equally good or better agreement with the *S* analysis than with the nongray *DP*(*S*) analysis. Some measured local irradiation results are more than three times the values obtained from the diffuse analysis. The predictions based on the nongray *DP*(*S*) model are lower than those based on the *S* model because the emission in the normal direction for metals is higher for the *CP* model than for the *DP* model. For the enclosure considered most of the energy emitted at oblique angles leaves the system without being absorbed, and mainly the energy emitted in the near normal directions contributes to irradiation. At the open end of the system, measured data depart significantly even from the *DP* analysis; the measurements are about 80 per cent higher.

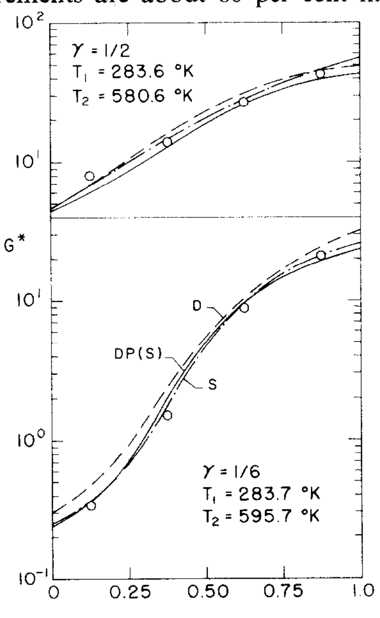

FIG. 5. Comparison between measured and predicted local irradiation for different models; surface arrangement *S-S-D*, $\delta = 1$, $\eta = \frac{3}{8}$.

For a system with "diffuse" surface 3($\sigma_m = 7{\cdot}1\,\mu$) and specular surfaces 1 and 2, the results are shown in Fig. 5. The predictions of all the analyses are very close. Even though surface 3 is not diffuse for the entire spectrum of incident radiation, there appear to be some compensating effects due to which the agreement of the *CP* analyses with the measured results is also good.

Some selected results for 'bidirectional' surface 3 ($\sigma_m = 0{\cdot}75\ \mu$) and specular surfaces 1 and 2 are presented in Fig. 6 only for $\eta = \frac{1}{8}$. For $\eta = \frac{3}{8}$ they are similar. The data follow the trend of the *B*(*D* + *S*) analysis. For a spacing of $\gamma = \frac{1}{6}$ the greatest discrepancy again occurs at the open end of the closed configuration where G^* based on the *B*(*D* + *S*) analysis is about 40 per cent lower than the measurements. The results of the *D* + *S* analysis are not shown in Fig. 6 for the sake of clarity, but are given in [8]. It is surprising that this simplified analysis agrees with the measurements even better than the detailed directional property analysis for $\gamma = \frac{1}{6}$.

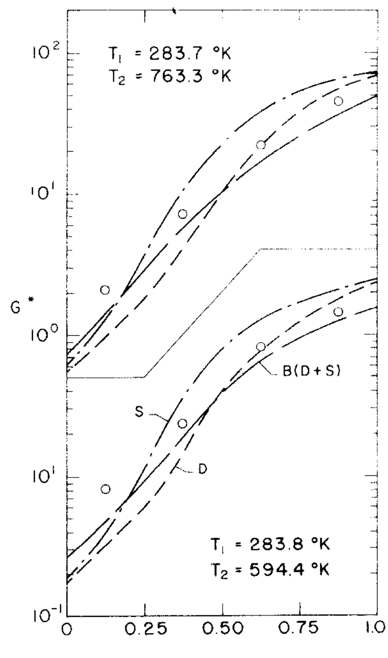

FIG. 6. Comparison between measured and predicted local irradiation for different models; surface arrangement *S-S-B*, $\delta = 1$, $\gamma = \frac{1}{6}$, $\eta = \frac{1}{8}$.

For "bidirectional" surface 2(σ_m = 1·5 μ), and with the other surfaces "specular", the results (Fig. 7) again show better agreement with the $B(D + S)$ analysis. The predictions are about 10–30 per cent lower than the data. The results based on diffuse analysis are as much as 70 per cent lower than the measurements. The $D + S$ analysis results are not shown in the figures but this simple analysis shows as good an agreement with the measurements as the more detailed $B(D + S)$ analysis, especially for $\gamma = \frac{1}{6}$.

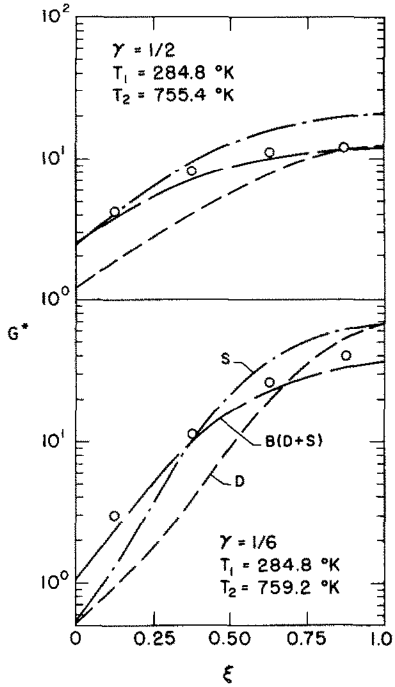

FIG. 7. Comparison between measured and predicted local irradiation for different models; surface arrangement S-B-S, $\delta = 1$, $\eta = \frac{1}{8}$

For an enclosure consisting of two "bidirectional" surfaces, and with $\gamma = \frac{1}{6}$, the data tend to fall more in line with the diffuse analysis. The results are in equally good agreement with the $B(D + S)$ as well as the D analysis, except at the open end of the system where they agree better with the former model. For $\gamma = \frac{1}{2}$ also the data (Fig. 8) agree equally well with the D as well as $B(D + S)$ analysis, but the S analysis always predicts higher irradiation. An enclosure with two bidirectional surfaces and a large γ spacing is expected to be more diffuse because the energy is incident at less oblique angles. The $D + S$ analysis is in equally good agreement with the measurements as the $B(D + S)$ analysis.

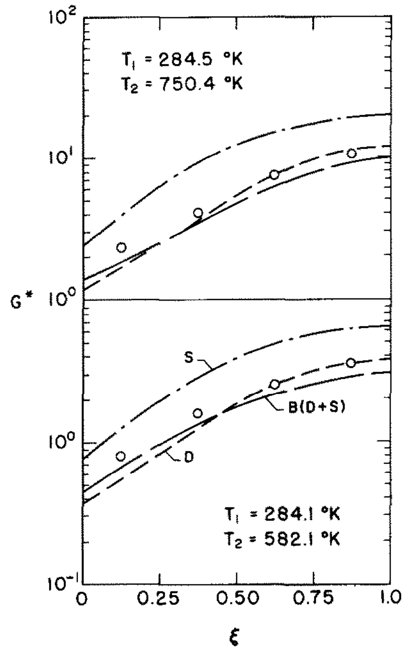

FIG. 8. Comparison between measured and predicted local irradiation for different models; surface arrangement S-B-B, $\delta = 1$, $\gamma = \frac{1}{2}$, $\eta = \frac{1}{8}$.

Total local irradiation has also been predicted on gray and semigray basis for models $DP(S)$ and $DP(D + S)$ but have not been included in the figures for the sake of clarity. The detailed tabulation of the results is given elsewhere [8]. Some sample results are presented in Fig. 9 which correspond to the same enclosure as in Fig. 6. In general it has been found that the gray and semigray $DP(S)$ and $DP(D + S)$ analyses are in reasonably good agreement with the data as well as the predictions based on correspond-

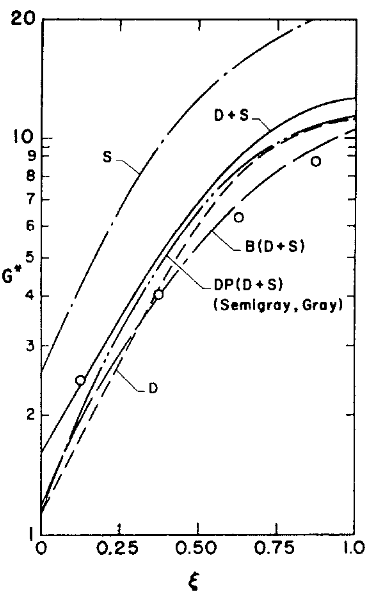

FIG. 9. Comparison between measured and predicted local irradiation for different models; surface arrangement S-S-B. $T_1 = 283{\cdot}9°K$, $T_2 = 756{\cdot}1°K$, $\delta = 1$, $\gamma = \frac{1}{2}$, $\eta = \frac{1}{8}$.

ing nongray calculations. This appears to be due to the fact that for highly reflecting materials the reflectance is not a strong function of wavelength in the infrared part of the spectrum for the temperature conditions in the experiments. These results emphasize that it is the directional effects which are more important.

Comparison of measurements and predictions on overall (average) basis

The results presented in Table 3 show that the constant property models (D, S, $D + S$, UR) are in better agreement with the measurements on an overall basis than on a local basis. The S analysis always overpredicts the irradiation. For a specular enclosure or when surface 3 is diffuse and others specular, the S analysis is within 10 per cent of the data. However, with bidirectional surfaces in the enclosure, the S analysis for some cases predicts G^* too high by as much as 120 per cent. In general, agreement of the D analysis with the measurements is better than that for the S analysis. Predictions with the $D + S$ model are closer to the experiments than the S analysis. Like the S analysis, the $D + S$ analysis also usually overpredicts the irradiation. Note that predictions of the $D + S$ analysis do not always lie between those of the D and S analyses, but the departure is small. The UR analysis yields equally good agreement with the experiments as the D analysis. The results reported by other investigators [22–25] for different systems are in substantial agreement with the findings of this study.

In contrast to the constant property S and $D + S$ analysis, the directional property analysis usually underpredicts the irradiation. Although the overall agreement of the DP analysis is better (within 20 per cent) than that of the CP analysis, it does not offer any significant advantage over the appropriate CP analysis. Also calculations with the nongray $B(D + S)$ or $DP(S)$ models do not yield better results than the corresponding semigray or gray analysis.

CONCLUSIONS

As a result of the present work the following conclusions may be drawn regarding local radiant heat transfer:

1. Analytical results indicate that the constant property diffuse and specular models do not yield the upper and lower bounds on local radiant heat flux.
2. Both constant property diffuse and specular models can fail badly. In general, the constant property specular analysis yields higher values of irradiation than the constant property diffuse analysis. The specularity of the surfaces must be considered for more accurate predictions.
3. A diffuse surface in the enclosure appears to destroy the effect of specularity of the other surfaces. Constant property and directional property analyses yield results which are in good agreement.
4. Semigray and gray analyses predict the irradiation reasonably well provided that the directional properties and the specu-

larity of the surfaces are taken into account.

5. The greatest discrepancy between the data and the analyses occurs at locations which are irradiated at oblique angles. It remains to be determined whether this discrepancy is due to the limitations of the analyses or the experiments.

The following conclusions can be drawn for evaluation of the overall (average) irradiation on total basis;

1. Calculation of the irradiation on a nongray basis does not yield improved results over the semigray or gray analyses.
2. The appropriate constant property models predict the irradiation reasonably well. The $D + S$ analysis provides better overall agreement with the data than the constant property diffuse or specular analyses.
3. The uniform (UR) and nonuniform (D) radiosity diffuse models are in satisfactory agreement with each other (within 20 per cent) and with the experimental data (within 45 per cent).

The conclusions drawn above were based on limited results for a particular combination of geometry, material and temperature levels. Therefore, care should be exercised in extending the results and conclusions to situations very much different from those studied here.

ACKNOWLEDGEMENTS

This research was sponsored by Manned Spacecraft Center, National Aeronautics and Space Administration, under contract No. NAS 9-8118 and was technically monitored by Mr. R. E. Durkee. Purdue Research Foundation provided financial support to J. S. Toor in the form of a David Ross Fellowship and Purdue University made available additional computer funds. The authors wish to acknowledge many helpful discussions with Prof. E. R. F. Winter during the initial phases of the work. Special appreciation is expressed to Prof. R. J. Schoenhals for his valuable comments.

REFERENCES

1. J. R. Schornhorst and R. Viskanta, An experimental examination of the validity of the commonly used methods of radiant heat transfer analysis, *J. Heat Transfer* **90C**, 429–436 (1968).
2. J. R. Howell and R. E. Durkee, Radiative transfer between surfaces in a cavity with collimated incident radiation: A comparison of analysis and experiment, *J. Heat Transfer* **93C**, 129–135 (1971).
3. J. S. Toor, R. Viskanta and E. R. F. Winter, Radiant heat transfer between simply arranged surfaces with direction dependent properties, AIAA Paper No. 69–624.
4. P. M. Engstrom, R. Viskanta and J. S. Toor, Study of radiation interchange in an enclosure consisting of plane isothermal and adiabatic surfaces, *Wärme- und Stoffübertragung* **3**, 63–69 (1970).
5. J. S. Toor and R. Viskanta, Experiment and analysis of directional effects on radiant heat transfer, *J. Heat Transfer* (accepted for publication).
6. J. S. Toor and R. Viskanta, A numerical experiment on radiant heat interchange by the Monte Carlo method, *Int. J. Heat Mass Transfer* **11**, 883–897 (1968).
7. J. R. Howell, Application of Monte Carlo to heat transfer problems, *Advances in Heat Transfer*, edited by J. Irvine and J. P. Hartnett, Vol. 5., pp. 1–54. Academic Press, New York (1968).
8. J. S. Toor, An experimental and analytical study of spectral and directional effects on radiant heat transfer, Ph.D. Thesis, Purdue University (1971).
9. J. R. Branstetter, Formulas for radiant heat transfer between nongray parallel plates of polished refractory metals, NASA TN D-2902 (1965).
10. H. E. Bennett and J. M. Bennett, Validity of the Drude theory, *Optical Properties and Electronic Structure of Metals and Alloys*, edited by F. Abeles, pp. 173–188. John Wiley, New York (1966).
11. B. A. Khrustalev, Radiative properties of solids, *Heat Transfer Sov. Res.* **2**, 149–170 (1970).
12. H. E. Bennett, Discussion on "Theoretical and experimental studies of the total emittance of metals", by W. J. Parker and G. L. Abbott, pp. 11–28, *Symposium on Thermal Radiation of Solids*, edited by S. Katzoff. NASA SP-55 (1965).
13. A. F. Houchens and R. G. Hering, Bidirectional reflectance of rough metal surfaces, *Progress in Aeronautics and Astronautics*, Vol. 20, pp. 65–90. Academic Press, New York (1967).
14. E. M. Sparrow and R. D. Cess, *Radiation Heat Transfer*. Brooks/Cole, Belmont, Calif. (1969). Calif. (1969).
15. P. Beckmann and A. Spizzichino, *The Scattering of Electromagnetic Waves from Rough Surfaces*. Macmillan, New York (1963).
16. R. C. Birkebak and E. R. G. Eckert, Effects of roughness of metal surfaces on angular distribution of monochromatic reflected radiation, *J. Heat Transfer* **87C**, 85–94 (1965).
17. T. F. Smith and R. G. Hering, Comparison of bidirectional reflectance measurements and model for rough metallic surfaces, *Proceedings of the Fifth Symposium on Thermophysical Properties*, edited by C. F. Bonilla, pp. 429–435. ASME, New York (1970).
18. J. R. Schornhorst and R. Viskanta, Effect of direction and wavelength dependent surface properties on radiant heat transfer, *AIAA Jl* **6**, 1450–1455 (1968).

19. R. P. Bobco, Analytical determination of radiation interchange factors, Hughes Aircraft Company, Space Systems Division, Report No. SSD 90190R (1968).
20. Y. S. Touloukian and D. P. DeWitt, Thermal radiation properties–metallic elements and alloys. *Thermophysical Properties of Matter*, Vol. 7. Plenum Press, New York (1970).
21. A. F. Houchens and R. G. Hering, Real surface effects on radiative heat transfer, Technical Report No. ME-TR-661-1, Department of Mechanical and Industrial Engineering, University of Illinois (1970).
22. B. Münch, Directional distribution in the reflection of heat radiation and its effect on heat transfer, NASA TT F-497 (1968).
23. J. T. Bevans *et al.*, Prediction of space vehicle thermal characteristics, Air Force Flight Dynamics Laboratory Technical Report No. AFFDL-TR 65-139 (1965).
24. T. J. Love and J. S. Gilbert, Experimental study of radiant heat transfer between parallel plates, Aerospace Research Laboratories Report No. ARL 66-0103 (1966).
25. E. Stammers, H. W. DenHartog and Wapenaar, Geometrical influences on the radiant heat transfer within an enclosed space, *Int. J. Heat Mass Transfer* **14**, 689–695 (1971).

ETUDE CRITIQUE DE LA VALIDITE DE MODELES SIMPLIFIES POUR L'ANALYSE DE TRANSFERT THERMIQUE PAR RAYONNEMENT

Résumé—On fait une critique de la validité des modèles simplifiés fréquemment utilisés pour estimer l'échange par rayonnement local aussi bien que global pour des surfaces réelles. Les effets directionnels et spectraux ont été étudiés par comparaison des résultats expérimentaux et des estimations basées sur six modèles simples pour les caractéristiques de rayonnement des surfaces. Les variations de propriété en direction ont été évaluées à partir des équations de Fresnel avec les constantes optiques prédites à l'aide de la théorie simple de Drude.

La configuration étudiée consiste en trois surfaces planes parallèles d'étendue finie. Ceci permet l'examen critique de l'influence de plusieurs paramètres sur l'échange par rayonnement. Les surfaces testées sont en or avec des rugosités dont la hauteur quadratique moyenne varie de 0.02 μ à 7.1 μ. Les températures de la surface varient de 77°K à 760°K. L'estimation de l'irradiation globale utilisant les modèles à propriété constante est en bon accord avec les résultats expérimentaux compte tenu des incertitudes expérimentales et théoriques. En général l'analyse et l'expérience s'accordent mieux pour la prédiction de l'irradiation locale quand on tient compte de la variation directionnelle et de la spécularité des surfaces. Les résultats expérimentaux sont également en bon accord avec les modèles à surfaces grises et non grises dans lesquelles les effets directionnels sont considérés et la composante spéculaire de réflectance indépendante de la direction est calculée en tenant compte des effets spectraux et directionnels.

EINE KRITISCHE ÜBERPRÜFUNG DER GÜLTIGKEIT VON VEREINFACHTEN MODELLEN ZUR BESTIMMUNG DES WÄRMEÜBERGANGES DURCH STRAHLUNG

Zusammenfassung—Die Gültigkeit der allgemein benutzten, vereinfachten Modelle zur Voraussage des lokalen und des gesamten Strahlungsaustausches zwischen realen Oberflächen wurde kritisch überprüft. Die richtungsabhängigen und die spektralen Effekte wurden untersucht, indem die experimentellen Ergebnisse mit den Voraussagen von sechs einfachen Modellen für die Strahlungscharakteristik von Oberflächen verglichen wurden. Die Änderungen der richtungsabhängigen Eigenschaften wurden mit den Fresnelschen Gleichungen berechnet, wobei die optischen Konstanten durch die einfache Drudesche Theorie gegeben waren. Die betrachtete Anordnung bestand aus drei planparallelen Oberflächen endlicher Ausdehung. Dadurch konnten die Einflüsse mehrerer Parameter auf den Strahlungsaustausch kritisch untersucht werden. Die Versuchsoberflächen waren aus Gold; der quadratische Mittelwert der Rauhigkeit reichte von 0.02 μm bis 7.1 μm. Die Temperatur der Umhüllung lag zwischen 77 K und 760 K. Der lokale einfallende Fluss wurde absolut gemessen. Innerhalb der kombinierten experimentellen und theoretischen Unsicherheiten stimmen die Voraussagen des gesamten Strahlungsflusses, die aus passenden Modellen mit konstanten Stoffwerten gewonnen wurden, gut mit den Experimenten überein. Im allgemeinen passen die Rechnung für den lokalen Strahlungsfluss und das Experiment besser zusammen, wenn die Änderungen der richtungsabhängigen Eigenschaften und die Spiegelung an den Oberflächen berücksichtigt werden. Die experimentellen Daten stimmen gleich gut mit Rechnungen für den grauen und halbgrauen Körper überein, bei denen die Richtungseffekte betrachtet werden und die richtungsunabhängige Spiegelkomponente der Reflexion durch Berücksichtigung der spektralen, richtungsabhängigen Effekte und der Konfigurationseinflüsse berechnet werden.

КРИТИЧЕСКИЙ АНАЛИЗ ПРИГОДНОСТИ УПРОЩЕННЫХ МОДЕЛЕЙ ДЛЯ ИЗУЧЕНИЯ ЛУЧИСТОГО ТЕПЛООБМЕНА

Аннотация—Критически анализируется пригодность общепринятых упрощенных моделей для расчета местного и общего лучистого теплообмена между реальными поверхностями. Эффекты напрвленности и спектральные эффекты исследовались путем сравнения экспериментальных данных и расчетов для шести простых моделей с излучающими поверхностями. Изменение свойств в зависимости от направления оценивалось по уравнениям Френеля, где оптические константы рассчитаны в соответствии с простой методикой Друда.

Рассматривались трехмерные параллельные поверхности конечного размера. Это позволяло провести критический анализ влияния различных параметров на лучистый обмен. Испытывались золотые поверхности со среднеквадратичной шероховатостью в пределах от 0,02 μ до 7,1 μ. Температуры ограждающей поверхности изменялись от 77°К до 760°К. Местный падающий поток измерялся по общепринятой методике. Расчеты общего излучения с помощью соответствующих моделей с постоянными свойствами находятся в хорошем соответствии с экспериментальными данными в пределах экспериментальной и теоретической погрешностей. В общем, анализ и эксперимент находятся в большем соответствии при расчете местного излучения, когда принимаются во внимание изменения свойств в зависимости от направления и зеркальности поверхностей. Экспериментальные данные также хорошо согласуются с данными анализа серых и полусерых поверхностей, когда рассматриваются эффекты направленности, а коэффициент направленного отражения, не зависимый от направления, рассчитывается с учетом спектральных эффектов, а также эффекта направленности и конфигурации.